

DISCLAIMER

This document was prepared as an account of work sponsored by the United States Government. While this document is believed to contain correct information, neither the United States Government nor any agency thereof, nor the Regents of the University of California, nor any of their employees, makes any warranty, express or implied, or assumes any legal responsibility for the accuracy, completeness, or usefulness of any information, apparatus, product, or process disclosed, or represents that its use would not infringe privately owned rights. Reference herein to any specific commercial product, process, or service by its trade name, trademark, manufacturer, or otherwise, does not necessarily constitute or imply its endorsement, recommendation, or favoring by the United States Government or any agency thereof, or the Regents of the University of California. The views and opinions of authors expressed herein do not necessarily state or reflect those of the United States Government or any agency thereof or the Regents of the University of California.

Coupled beam hose and self-modulation instabilities in overdense plasma

C. B. Schroeder,¹ C. Benedetti,¹ E. Esarey,¹ F. J. Gr ner,² and W. P. Leemans¹

¹*Lawrence Berkeley National Laboratory, Berkeley, California 94720, USA*

²*Universit t Hamburg, Luruper Chaussee 149, 22761 Hamburg, Germany*

(Dated: August 2, 2012)

Abstract

Transverse stability of the drive beam is critical to plasma wakefield accelerators. A long, relativistic particle beam propagating in an overdense plasma is subject to beam envelope modulation and centroid displacement (hosing) instabilities. Coupled equations for the beam centroid and envelope are derived and solved. It is shown that the hosing growth rate is comparable to self-modulation, and coupling of the self-modulation enhances beam hosing and induces harmonic content. Large amounts of hosing can significantly alter the structure of the plasma wakefields.

PACS numbers: 52.40.Mj, 52.35.-g

I. INTRODUCTION

Plasma-based accelerators [1] are considered a candidate technology for the next generation colliders to expand the energy frontier of high energy physics experiments [2]. Plasma-based acceleration is realized by using an intense laser [1] or charged-particle beam [3–5] to excite large amplitude electron plasma waves with relativistic phase velocity. The electric field amplitude of the plasma wave (space-charge oscillation) can be several orders of magnitude greater than conventional accelerators, on the order of $E_0 = cm_e\omega_p/e$, or $E_0[\text{V/m}] \simeq 96\sqrt{n_0[\text{cm}^{-3}]}$, where $\omega_p = (4\pi n_0 e^2/m_e)^{1/2}$ is the plasma frequency, n_0 is the ambient electron number density, m_e and e are the electron rest mass and charge, respectively, and c is the speed of light in vacuum.

It has been proposed to use a highly relativistic proton beam, such as those available at CERN (European Organization for Nuclear Research), to drive a plasma accelerator [6, 7], effectively using the plasma to transfer energy from the proton beam to a lepton beam. Efficient plasma wave excitation requires beam drivers with spatial structure on the scale of the plasma skin depth, and compact, high-gradient plasma accelerators (i.e., high plasma density) require short drive beams. Generating short proton beams (or proton beams with spatial structure at the plasma frequency) is challenging, for interesting plasma densities, and it has been proposed to rely on a beam-plasma instability to modulate the beam at the plasma wavelength $\lambda_p = 2\pi c/\omega_p$, driving a large amplitude wave [8–10]. The growth and phase velocity of the self-modulation instability has been studied in Refs. [11, 12]. Tapered plasmas may be considered to control the phase velocity of the self-modulated beam-driven plasma wave, although sufficiently large background density variations will suppress the instability [13]. Proof-of-principle experiments to study the physics of beam self-modulation using lepton beams have also been proposed [14].

Transverse stability of the drive particle beam is a major concern for the development of the beam-driven plasma wakefield accelerator (PWFA), and particularly for drive beams longer than the plasma skin depth (such as in the proposed self-modulated proton-driven PWFA). In this work we examine the hosing instability of a long drive beam undergoing self-modulation in an overdense plasma. Beam hosing, a type of transverse two-stream instability, is the result of the feedback between a head-to-tail centroid displacement with respect to the propagation direction and the excited plasma wakefield that leads to growth

in the beam centroid displacement. Previous work on beam hosing in plasma has focused on the underdense regime where the beam density is large compared to the plasma density $n_b \gg n_0$ (where n_b is the beam density), and both the long-beam (adiabatic, ion-channel) regime ($k_p L_b \gg 1$) [15] and the nonlinear short-bunch ($k_p L_b < 1$) blow-out regime [16] has been examined. Future proton-driven PWFA experiments will be in the overdense regime where $n_b \ll n_0$. Whittum [17] considered the transverse two-stream instability in the overdense regime assuming a rigid beam model. Here we derive and solve the coupled beam envelope and centroid equations self-consistently driven by the beam-excited plasma wave in the overdense regime. It was suggested in Ref. [8] that the self-modulation instability grows much faster than the hosing instability and that the self-modulation may alleviate the effects of hosing. In this work we calculate the hosing growth rate including return current effects (where the beam radius is of order the plasma skin depth k_p^{-1}). The growth rate for beam hosing in the long-beam, strongly-coupled overdense regime is comparable to that of the self-modulation instability. It is also shown that the coupling of the beam envelope modulations enhances the growth of the beam centroid displacements. A similar coupling between laser hosing and self-modulation can also occur for long laser pulses propagating in underdense plasma [18].

II. BEAM CENTROID EVOLUTION

The wakefield generated by a relativistic charged particle beam moving through an overdense, initially neutral, plasma can be calculated using the quasi-static, cold plasma fluid and Maxwell equations assuming $n_b < n_0$. The evolution of the normalized wake potential $\psi = e(\Phi - A_z)/m_e c^2$ (with Φ the electrostatic and A_z the axial vector potentials) of the quasi-static beam-driven plasma wave is given by

$$(\partial_\zeta^2 + 1) (\nabla_\perp^2 - 1) \psi = -(q/e)n_b/n_0, \quad (1)$$

where q is the charge of the beam particle with beam density n_b , and $\zeta = k_p(z - \beta_b t)$ is the normalized co-moving variable with $k_p = \omega_p/c$ and $v_b = c\beta_b$ is the drive beam velocity. We have assumed a highly-relativistic drive beam such that $\gamma = (1 - \beta_b^2)^{-1/2} \gg 1$ and that the background plasma ions are immobile on the time scales of interest [19]. In the following all length scales are normalized to the plasma skin depth k_p^{-1} . The force on a relativistic beam

from the plasma wave is given by the wake potential $\mathbf{F}/(eE_0) = -(q/e)\nabla\psi$.

Consider a general (axisymmetric) transverse beam density distribution with a small centroid offset in the x -direction:

$$n_b \left(\sqrt{[x - x_c]^2 + y^2} \right) \simeq n_{b0} - (\partial_r n_{b0}) x_c \cos \theta, \quad (2)$$

where $n_{b0} = n_b(x, y, x_c = 0) = n_b(r)$. Note that the charge per unit length in a beam slice is conserved with the centroid displacement. Given the general beam distribution $n_b = \sum_m \hat{n}_m \cos(m\theta)$, the wake potential may be written as $\psi = -(q/e) \sum_m \hat{\psi}_m \cos(m\theta)$ satisfying

$$(\partial_\zeta^2 + 1) [\partial_r^2 + (1/r)\partial_r - m^2/r^2 - 1] \hat{\psi}_m = \hat{n}_m/n_0 \quad (3)$$

with the Green function solution

$$\hat{\psi}_m = \int_\infty^\zeta d\zeta' \sin(\zeta - \zeta') \int_0^\infty r' dr' K_m(r_>) I_m(r_<) \frac{\hat{n}_m}{n_0}, \quad (4)$$

where $r_< (r_>)$ is the smaller (larger) of r and r' . The force provided by the beam-excited plasma wave along the centroid displacement is $F_x/(eE_0) = -(q/e)\partial_x\psi$.

The evolution equation for the centroid $x_c = \langle x \rangle$ of any beam slice (ζ) is

$$\frac{d^2 x_c}{dz^2} = -(q/e) \frac{m_e}{\gamma M_b} \langle \partial_x \psi \rangle, \quad (5)$$

where M_b is the mass of the beam particle and the brackets indicate an average over the transverse distribution. Averaging the transverse force over the beam distribution Eq. (2) yields the equation for the centroid evolution

$$\frac{d^2 x_c}{dz^2} + x_c \frac{m_e}{\gamma M_b} \frac{\int_0^\infty r dr (\partial_r n_{b0}) (\partial_r \hat{\psi}_0)}{2 \int_0^\infty r dr (n_{b0})} = \frac{m_e}{\gamma M_b} \frac{\int_0^\infty dr (n_{b0}) [\partial_r (r \hat{\psi}_1)]}{2 \int_0^\infty r dr (n_{b0})} \quad (6)$$

for any general axisymmetric beam distribution n_{b0} . Note that, to order $\mathcal{O}(x_c/\langle x^2 \rangle^{1/2})$ a cylindrically-symmetric distribution will remain cylindrically-symmetric $\langle (x - x_c)^2 \rangle(z) = \langle y^2 \rangle(z)$. Assuming a flat-top transverse distribution with a centroid perturbation, i.e., $n_b = \hat{n}_b(r_{b0}/r_b)^2 \Theta(r_b - \sqrt{[x - x_c]^2 + y^2})$, Eq. (6) may be evaluated to yield the centroid $x_c(\zeta, z)$ evolution equation at any beam slice (ζ) in the long beam (i.e., neglecting initial longitudinal beam density variations) adiabatic regime:

$$\frac{d^2 x_c}{dz^2} = \frac{k_b^2}{\gamma} \frac{I_1(r_b)}{r_b} \int_\infty^\zeta d\zeta' \sin(\zeta - \zeta') \frac{r_{b0}^2}{r_b(\zeta')} K_1(r_b(\zeta')) [x_c(\zeta') - x_c(\zeta)], \quad (7)$$

where $k_b^2 = 4\pi\hat{n}_b e^2 / M_b c^2$ is the beam wavenumber and $r_b(\zeta, z)$ is the beam radius. Equation (7) indicates that a beam tilt or nonuniform head-to-tail displacement with respect to the beam propagation direction $x_c(\zeta) \neq x_c(\zeta')$ is required for the hose instability. This is similar to the centroid equation describing laser hosing for which a head-to-tail centroid non-uniformity is also required for instability [18]. One consequence is that axis-symmetric beams should be stable to hosing, and observation of hosing in particle-in-cell codes that load axis-symmetric beams is unphysical and the result of numerical noise in the algorithm and from the finite number of macro-particles.

If the beam envelope is non-evolving $r_b = r_0 = \text{constant}$, i.e., a rigid beam approximation valid for a long beam without a seed for the self-modulation instability, Eq. (7) can be linearized to yield

$$(\partial_\zeta^2 + 1)(\partial_z^2 + \mu\hat{k}_\beta^2)x_c = \mu\hat{k}_\beta^2 x_c, \quad (8)$$

where $\mu = 2I_1(r_0)K_1(r_0)$ and $\hat{k}_\beta = (k_b/k_p)(2\gamma)^{-1/2}$. In the narrow beam limit $r_0 \ll 1$, $\mu \simeq 1 - (0.366 + \ln[1/r_0])r_0^2/2$. The factor $\mu(r_0)$ describes the plasma return current; for $r_0 \sim 1$, the plasma return current partially flows through the bulk of the beam neutralizing the current, reducing the focusing [20] and instability coupling. In the long-beam, early-time regime such that $|\zeta| \gg \hat{k}_\beta z$ (i.e., $|\partial_z \hat{x}_c| \gg \hat{k}_\beta$ and $|\partial_\zeta \hat{x}_c| \ll 1$), Eq. (8) yields

$$(\partial_\zeta \partial_z^2 + i\mu\hat{k}_\beta^2/2)\hat{x}_c = 0, \quad (9)$$

where \hat{x}_c is a slowly-varying envelope of the centroid displacement: $x_c = (\hat{x}_c/2)\exp(i\zeta) + \text{c.c.}$. Consider the initial conditions, $\hat{x}_c(z, \zeta = 0) = \delta_c \Theta(z)$, $\hat{x}_c(z = 0, \zeta) = \delta_c$, and $\partial_z \hat{x}_c(z = 0, \zeta) = 0$, which correspond to a beam with slice-to-slice centroid fluctuations with a Fourier component at k_p with amplitude δ_c . Using standard Laplace transform techniques, and applying the method of steepest descents, yields the asymptotic solution

$$x_c = \delta_c \left[\frac{3^{1/4}}{(8\pi)^{1/2}} \right] \frac{e^{N_h}}{N_h^{1/2}} \cos\left(\pi/12 - k_p \zeta - N_h/\sqrt{3}\right), \quad (10)$$

where the number of e-folds of the hose instability is

$$N_h = (3^{3/2}/4) \left(\mu\hat{k}_\beta^2 \zeta z^2 \right)^{1/3}. \quad (11)$$

Note that a similar growth rate was derived in Ref. [17] for a rigid beam with a Bennett profile. In general, the instability will be weakly dependent on the initial transverse beam distribution, and the growth rate Eq. (11) (calculated assuming a flat-top distribution) will

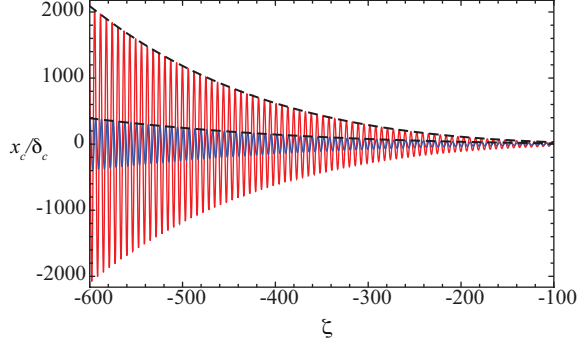


FIG. 1. (Color online) Centroid displacement x_c from numerical solution of Eq. (7) versus ζ after propagating $\hat{k}_\beta z = 0.81$ (blue curve) and $\hat{k}_\beta z = 1.1$ (red curve), and amplitude of the asymptotic solution Eq. (10) (dashed lines) for a 450 GeV proton beam with $\hat{n}_b/n_0 = 0.008$ and $r_0 = 1$.

be modified by a constant of order unity. For example, if a parabolic beam distribution (with equal charge and rms radius) is assumed, the hosing growth rate is $N_{\text{parabolic}}/N_h = 2/3^{2/3}$ for $r_0 \ll 1$.

Comparing the hosing growth rate to the self-modulation instability growth rate [11], $N_{\text{smi}} = (3^{3/2}/4)(2\nu\hat{k}_\beta^2\zeta z^2)^{1/3}$ with $\nu = 4I_2(r_0)K_2(r_0)$, one finds $N_h/N_{\text{smi}} = (\mu/2\nu)^{1/3} \sim 1$. In the narrow beam limit $r_0 \ll 1$, $N_h/N_{\text{smi}} = 2^{-1/3}$. In contrast to the predictions of Ref. [8], the growth of the beam hosing instability is comparable to that of the beam self-modulation.

Figure 1 shows the centroid displacement given by the numerical solution of Eq. (7) versus distance behind the head of the beam (head of beam at $\zeta = 0$) after propagating $\hat{k}_\beta z = 0.81$ (blue curve) and $\hat{k}_\beta z = 1.1$ (red curve). Also shown in Fig. 1 is the amplitude of the asymptotic solution Eq. (10) (dashed lines). Here we considered evolution of a 450 GeV proton beam ($\gamma = 480$), with $\hat{n}_b/n_0 = 0.008$ and $r_0 = 1$ ($\mu \simeq 0.68$), propagating in a $n_0 = 10^{15} \text{ cm}^{-3}$ plasma, i.e., $\simeq 180 \text{ } \mu\text{m}$ spot size, $\simeq 12 \text{ cm}$ bunch length, and 10^{11} particles (beam parameters near that of the CERN Super Proton Synchrotron). There is excellent agreement between the numerical solution of Eq. (7) and the linear hosing growth rate Eq. (11).

III. COUPLED BEAM CENTROID AND RADIUS EVOLUTION

Now we will consider the influence of the beam envelope modulations on the hose instability, coupled via the wakefield. For a small centroid displacement, such that only the dipole mode is retained as in Eq. (2), the beam envelope may be described by the rms radius. For higher-order centroid displacements (beyond the dipole), asymmetry arises and the beam becomes elliptical, i.e., $\langle (x - x_c)F_x \rangle = \langle yF_y \rangle + \mathcal{O}(x_c/r_b)^2$ for $|x_c| < r_b$. In the limit of small centroid perturbations compared to the beam radius, i.e., correct to order $\mathcal{O}(x_c/r_b)$, the evolution equation for the beam radius at any slice ζ is

$$\frac{d^2 r_b}{dz^2} - \frac{\epsilon^2}{r_b^3} = \frac{m_e}{\gamma M_b} \frac{2}{r_b} \frac{\int_0^\infty dr n_{b0} r^2 \partial_r \hat{\psi}_0}{\int_0^\infty r dr (n_{b0})}, \quad (12)$$

where ϵ is the geometric emittance. Assuming a flat-top transverse beam distribution, in the long beam regime, Eq. (12) yields [11]

$$\frac{d^2 r_b}{dz^2} - \frac{\epsilon^2}{r_b^3} = -\frac{k_b^2}{\gamma} \frac{4I_2(r_b)}{r_b} \int_\infty^\zeta d\zeta' \sin(\zeta - \zeta') \frac{r_{b0}^2}{r_b} K_1(r_b). \quad (13)$$

The beam radius evolution $r_b(\zeta, z)$ via Eq. (13) couples to the centroid evolution Eq. (7). Note that, in this small displacement, dipole approximation the beam radius evolution is independent of the centroid perturbation. This is similar to the case of laser hosing for which the radius equation is independent of the laser centroid for small centroid displacements [18]. The laser centroid depends on the laser radius, but in a much different form than for the particle beam case.

The initial seed for the radial modulation and centroid displacement can be due to beam mis-alignments, beam transport errors, or any asymmetries in the beam creation and delivery. Neglecting these non-ideal beam effects, the finite number of beam particles (i.e., schottky noise) will generate a seed for the instabilities. Consider an axis-symmetric beam containing N particles. At any slice of the beam, the initial beam radius may be expressed as $r_b(\zeta, z=0)/r_0 = 1 + \sigma_e$ and the initial centroid displacement as $x_c(\zeta, z=0)/r_0 = \sigma_c$, where σ_e and σ_c are random perturbations due to the finite number of beam particles. For a beam slice containing $N_s \gg 1$ particles, the expectation for the deviation from the mean is $[\overline{\sigma_c^2(\zeta)}]^{1/2} = [\langle x^2 \rangle^{1/2}/r_0]/\sqrt{N_s}$ for the centroid displacement and $[\overline{\sigma_e^2(\zeta)}]^{1/2} = [\langle x^4 \rangle^{1/2}/2\langle x^2 \rangle]/\sqrt{N_s}$ for the beam radius, or $[\overline{\sigma_c^2(\zeta)}]^{1/2} \sim [\overline{\sigma_e^2(\zeta)}]^{1/2} \sim 1/\sqrt{N_s}$. Here the bar indicates the ensemble average over the random distributions of beam particles

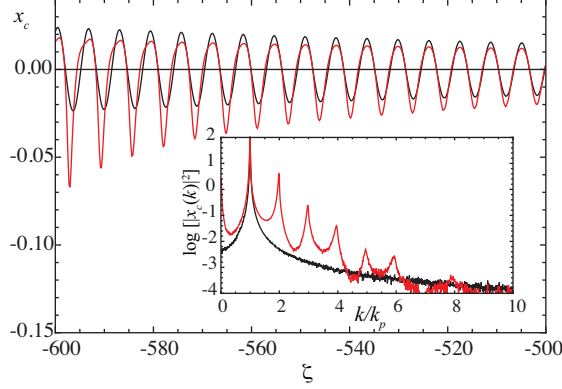


FIG. 2. (Color online) Numerical solution for the growth of the centroid displacement Eq. (7) without (black curves) and with (red curves) seeding the self-modulation at $\hat{k}_\beta z = 1.14$. The seed was random with standard deviation 10^{-4} . Beam-plasma parameters are a 450 GeV proton beam with $\hat{n}_b/n_0 = 0.008$, $k_p r_0 = 1$, and head of beam at $\zeta = 0$. The inset shows the spectrum of x_c in $\zeta \in [-600, 0]$ for the cases without (black curve) and with (red curve) seeding the envelope modulation.

in the slice. To model the beam we consider a discretization that represents the beam as $L/\Delta\zeta$ slices, such that $N_s \sim N/(L/\Delta\zeta)$. For $N \sim 10^{11}$ and $L/\Delta\zeta \sim 10^3$, the expectation for the amplitude of the fluctuations in beam centroid and radius owing to the finite number of beam particles is $[\overline{\sigma_c^2(\zeta)}]^{1/2} \sim [\overline{\sigma_e^2(\zeta)}]^{1/2} \sim 10^{-4}$.

Figure 2 shows numerical solutions for the growth of the centroid perturbation Eq. (7) with self-consistent modulation of the beam envelope Eq. (13), for the same beam-plasma parameters as Fig. 1 (head of beam at $\zeta = 0$) after propagating $\hat{k}_\beta z = 1.14$. The initial beam radius at any beam slice was $r_b(\zeta, z = 0) = 1 + \sigma_e$, where $r_0 = 1$ is the long-beam equilibrium radius [11], and the initial centroid displacement at any slice was $x_c(\zeta, z = 0) = \sigma_c$. The black curve shows the centroid displacement with initial random perturbations with standard deviation $[\overline{\sigma_c^2(\zeta)}]^{1/2} = 10^{-4}$ and $\sigma_e = 0$ (i.e., no seed for the envelope modulation), and the red curve shows the centroid displacement with initial random perturbations having standard deviation $[\overline{\sigma_c^2(\zeta)}]^{1/2} = [\overline{\sigma_e^2(\zeta)}]^{1/2} = 10^{-4}$ (i.e., seeding both modulation and hosing instabilities). The inset shows the spectrum of the centroid displacements in the region $\zeta \in [-600, 0]$. The coupling of the envelope modulation to the hosing is evident in the harmonic generation present in the centroid perturbation when the modulation instability

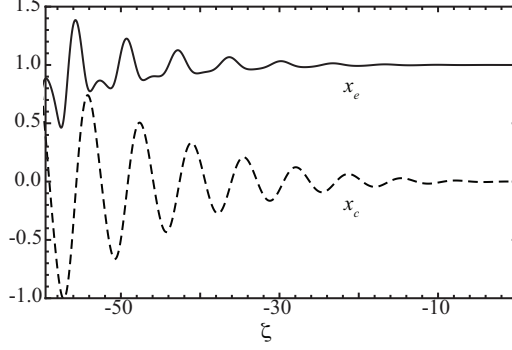


FIG. 3. Beam envelope x_e and centroid x_c versus ζ at $k_b z / \gamma^{1/2} = 4$ for an initial perturbation of 10^{-4} in the envelope and 10^{-3} in the centroid, assuming a slab proton beam with $\gamma = 480$ and $n_b/n_0 = 0.008$.

is seeded. Note also a DC component is present, indicating a long wavelength displacement of the beam tail from the axis.

As shown in Fig 2 larger centroid perturbations occurred with coupling of the hosing and self-modulation instabilities, for the initial random seed used in Fig. 2. Averaging over many realizations of initial random seeds, with the same beam-plasma parameters as Fig. 2, the maximum displacement was $\langle \langle \max[x_c(\zeta), (\overline{\sigma_e^2})^{1/2} = 10^{-4}] \rangle \rangle / \langle \langle \max[x_c(\zeta), \sigma_e = 0] \rangle \rangle \simeq 2.2$ at $\hat{k}_\beta z = 1.14$ observed in the region $\zeta \in [-600, 0]$, i.e., the average centroid displacement with seeding of the envelope modulations is larger than without seeding ($\sigma_e = 0$). The coupling of the self-modulation to the hosing not only generates harmonics, but, in general, will increase the amplitude of beam hosing.

The above analysis assumed a small beam displacement $x_c < r_b$. To understand the phenomenology of the coupling of the centroid to the beam envelope modulation, we considered the coupled envelope and centroid evolution equations in 2D-cartesian (x, z) geometry (i.e., a flat beam), valid for arbitrarily large centroid displacements. The solution for the wake potential in 2D-cartesian geometry is

$$\psi = -\frac{q}{e} \int_{-\infty}^{\zeta} d\zeta' \sin(\zeta - \zeta') \int_{-\infty}^{\infty} \frac{dx'}{2} e^{x_{<} - x_{>}} \frac{n_b(x')}{n_0}, \quad (14)$$

where $x_{<}$ ($x_{>}$) is the smaller (larger) of x and x' . For a flat-top beam transverse distribution $n_b = \hat{n}_b(x_0/x_e)\Theta[x_e - (x - x_c)]$, the evolution of the beam envelope and centroid are, in the long beam regime,

$$\begin{aligned} \frac{d^2 x_e}{dz^2} - \frac{9\epsilon_x^2}{x_e^3} &= \frac{k_b^2}{\gamma} \frac{3x_c}{x_e^2} \sinh(x_e) \int_{-\infty}^{\zeta} d\zeta' \sin(\zeta - \zeta') \frac{x_0 e^{-x_e(\zeta')}}{x_e(\zeta')} \sinh[x_c - x_c(\zeta')] \\ &- \frac{k_b^2}{\gamma} \frac{3}{x_e} \left[\cosh(x_e) - \frac{\sinh(x_e)}{x_e} \right] \int_{-\infty}^{\zeta} d\zeta' \sin(\zeta - \zeta') \frac{x_0}{x_e(\zeta')} e^{-x_e(\zeta')} \cosh[x_c - x_c(\zeta')], \end{aligned} \quad (15)$$

and

$$\frac{d^2 x_c}{dz^2} = -\frac{k_b^2}{\gamma} \frac{\sinh(x_e)}{x_e} \int_{-\infty}^{\zeta} d\zeta' \sin(\zeta - \zeta') \frac{x_0}{x_e(\zeta')} e^{-x_e(\zeta')} \sinh[x_c(\zeta) - x_c(\zeta')], \quad (16)$$

respectively, where ϵ_x is the rms slice geometric emittance. In the limit of a small beam centroid displacement $x_c < x_e \sim 1$, the beam centroid couples to the envelope evolution to order $\mathcal{O}(x_c/x_e)^2$. Hence we expect 2nd harmonic generation in the envelope modulation owing to the coupling to the centroid displacement. Figure 3 shows the numerical solution to the coupled beam envelope and centroid Eqs. (16) and (15) for a proton beam [initially in equilibrium $x_e(z=0) = 1$] with $\gamma = 480$ and $n_b/n_0 = 0.008$. Here we have assumed an initial seed amplitude of 10^{-4} for the envelope modulation and 10^{-3} for the centroid displacement. As illustrated in Fig. 3, when the centroid displacement grows large $x_c \sim x_e \sim 1$, the envelope perturbation develops modulation at $\lambda_p/2$.

For large beam centroid displacements on the order of the plasma skin-depth, $x_c \sim 1$, the structure of the beam-driven wakefields is strongly modified, which will have deleterious

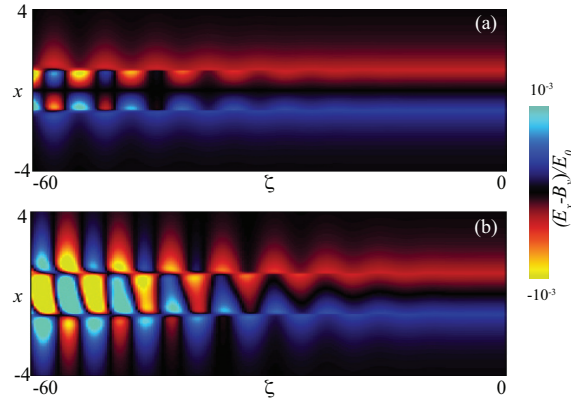


FIG. 4. (Color online) Transverse wakefield $(E_x - B_y)/E_0$ after $k_b z/\gamma^{1/2} = 4$ with the same beam-plasma parameters as Fig. 3, for (a) seeding only the envelope modulations (an initial perturbation of 10^{-4}) and (b) an initial seed of 10^{-4} in the envelope modulation and 10^{-3} in the centroid displacement.

effects for acceleration. Figure 4 shows the transverse wake $(E_x - B_y)/E_0$ calculated by solving the coupled Eqs. (16) and (15) for the same beam-plasma parameters as Fig. 3 after propagating $k_b z / \gamma^{1/2} = 4$ for (a) without seeding the centroid perturbation (initial envelope perturbation of 10^{-4}) and (b) with seeding both the centroid and envelope perturbations (10^{-4} in the envelope and 10^{-3} in the centroid). Figure 4(b) shows that the hosing instability will generate an on-axis deflecting force that will scatter a trailing witness bunch.

IV. CONCLUSIONS

In this work we have derived the coupled beam envelope (self-modulation) and centroid (hosing) equations for a long beam in an overdense plasma. The growth rate of the hosing was calculated including return current effects. The hosing growth is comparable to the growth of the beam envelope self-modulation $N_h/N_{\text{smi}} \sim 1$. The coupling between the beam centroid displacement and envelope modulations results in harmonic generation in the centroid displacements, and, in general, larger amplitude hosing. Sufficiently large centroid displacements results in coupling to the envelope modulations and strong modification of the wakefield, as demonstrated by solving the coupled equations in 2D-cartesian geometry. Transverse beam stability is critical to PWFAs, and these results indicate the necessity for strongly seeding the self-modulation instability without seeding beam hosing for future self-modulated PWFA experiments.

ACKNOWLEDGMENTS

The authors would like to thank J. Osterhoff and F. Stephan for useful discussions. This work was supported by the Director, Office of Science, Office of High Energy Physics, of the U.S. Department of Energy under Contract No. DE-AC02-05CH11231.

-
- [1] E. Esarey, C. B. Schroeder, and W. P. Leemans, *Rev. Mod. Phys.* **81**, 1229 (2009).
 - [2] C. B. Schroeder *et al.*, *Phys. Rev. ST Accel. Beams* **13**, 101301 (2010).
 - [3] P. Chen *et al.*, *Phys. Rev. Lett.* **54**, 693 (1985).
 - [4] J. B. Rosenzweig *et al.*, *Phys. Rev. Lett.* **61**, 98 (1988).

- [5] I. Blumenfeld *et al.*, Nature **445**, 741 (2007).
- [6] A. Caldwell *et al.*, Nature Phys. **5**, 363 (2009).
- [7] K. V. Lotov, Phys. Rev. ST Accel. Beams **13**, 041301 (2010).
- [8] N. Kumar, A. Pukhov, and K. Lotov, Phys. Rev. Lett. **104**, 255003 (2010).
- [9] K. V. Lotov, Phys. Plasmas **18**, 024501 (2011).
- [10] A. Caldwell and K. V. Lotov, Phys. Plasmas **18**, 103101 (2011).
- [11] C. B. Schroeder *et al.*, Phys. Rev. Lett. **107**, 145002 (2011).
- [12] A. Pukhov *et al.*, Phys. Rev. Lett. **107**, 145003 (2011).
- [13] C. B. Schroeder *et al.*, Phys. Plasmas **19**, 010703 (2012).
- [14] J. Vieira *et al.*, Phys. Plasmas **19**, 063105 (2012).
- [15] D. H. Whittum *et al.*, Phys. Rev. Lett. **67**, 991 (1991).
- [16] C. Huang *et al.*, Phys. Rev. Lett. **99**, 255001 (2007).
- [17] D. H. Whittum, Phys. Plasmas **4**, 1154 (1997).
- [18] P. Sprangle, J. Krall, and E. Esarey, Phys. Rev. Lett. **73**, 3544 (1994).
- [19] J. B. Rosenzweig *et al.*, Phys. Rev. Lett. **95**, 195002 (2005).
- [20] R. Govil *et al.*, Phys. Rev. Lett. **83**, 3202 (1999).